Computers and Concrete, *Vol. 24, No. 5 (2019) 445-452*
DOI: https://doi.org/10.12989/cac.2019.24.5.445

Dynamic stress, strain and deflection analysis of pipes conveying nanofluid buried in the soil medium considering damping effects subjected to earthquake load

M. Heydari Nosrat Abadi*, H. Hassanpour Darvishi and A.R. Zamani Nouri

Department of Civil Engineering, Engineering and Management of Water Resources, Shahr-e-Qods Branch, Islamic Azad University, Tehran, Iran

(*Received April 6, 2019, Revised October 8, 2019, Accepted October 11, 2019*)

Abstract. In this paper, dynamic stress, strain and deflection analysis of concrete pipes conveying nanoparticles-water under the seismic load are studied. The pipe is buried in the soil which is modeled by spring and damper elements. The Navier-Stokes equation is used for obtaining the force induced by the fluid and the mixture rule is utilized for considering the effect of nanoparticles. Based on refined two variables shear deformation theory of shells, the pipe is simulated and the equations of motion are derived based on energy method. The Galerkin and Newmark methods are utilized for calculating the dynamic stress, strain and deflection of the concrete pipe. The influences of internal fluid, nanoparticles volume percent, soil medium and damping of it as well as length to diameter ratio of the pipe are shown on the dynamic stress, strain and displacement of the pipe. The results show that with enhancing the nanoparticles volume percent, the dynamic stress, strain and deflection decrease.

Keywords: dynamic response; soil medium; fluid; damping; nanoparticles

1. Introduction

Due to the important application of concrete pipes in different industries, investigation of the dynamic stress, strain and deflection of them subjected to earthquake loads is one of the interest topics among the researchers. In this paper, seismic analysis of concrete pipes in the soil medium with nanoparticles-water fluid internal flow under the earthquake load is studied (El-Helou and Aboutaha 2015, Hind *et al*. 2016, Liu *et al*. 2018).

In the literature, there are many works in the field of dynamic analysis of structure subjected to earthquake load. Dynamic response of the structures has been reported by many researchers. Powell (1978) presented seismic analysis of cross-country and above-ground pipes based on numerical methods. O'Leary and Datta (1985) studied the dynamic stresses of the pipelines buried in the soil subjected to seismic load utilizing the numerical methods. Belardinelli *et al*. (2003) calculated of dynamic and static stresses in spring-slider system under the seismic load. Kumar Mishra *et al*. (2013) used base isolation as an effective control strategy for improving seismic performance of structures. Wu *et al*. (2015) used the beam theory and the spectrum method to dynamic analysis of oil pipeline under the earthquake load. Allahdadian and Boroomand (2016) presented the optimization analysis of planar frames subjected to seismic load based on a numerical method. Kayen (2017) investigated the dynamic deflection of the marine sediment in the seismic environment. Optimization and seismic response of water tank reinforced by internal baffle rings were presented by Zhao *et al*. (2017). A refined Frequency Domain Decomposition algorithm with Non-parametric structural system identification was used by Pioldi *et al*. (2017) to evaluate the properties of civil engineering buildings subjected to earthquake excitation. Ding *et al*. (2018) worked on the underwater table shaking under wave-current and earthquake loads. Peng *et al*. (2018) developed a modified unscented Kalman filter (MUKF) algorithm for estimating dynamic positioning ship motion states. Karimirad and Michailides (2018) examined the dynamic response of the *V*-shaped semisubmersible under different possible fault conditions.

Mathematical modeling of the concrete structures is an interesting topic. For example, vibration and instability of carbon nanotubes (CNTs) and Fe_2O_3 nanoparticles-reinforced-concrete pipes with internal fluid flow were investigated by Zamani-Nouri (2017). Heydari Nosrat Abadi and Zamani Nouri (2018a) studied critical fluid velocity in temperature-dependent pipes conveying fluid mixed with nanoparticles using higher order shear deformation theory. Vibration analysis in the pipes made from concrete located in the soil with internal fluid flow was presented by Zamani Nouri (2018b). Zamani Nouri (2018c) the dynamic analysis of the pipes made from concrete with internal fluid flow buried by soil was presented.

To the best of author knowledge, dynamic analysis of concrete pipes internal water-nanoparticles is studied. The pipe is buried in the soil medium modeled by spring and damper elements. The pipe is modeled by higher order shear deformation theory of shells and the equations of

*Corresponding author, Post Graduate Student
E-mail: mohammadheydari.n1994@gmail.com

http://www.techno-press.org/?journal=cac&subpage=8
ISSN: 1598-8198 (Print), 1598-818X (Online)

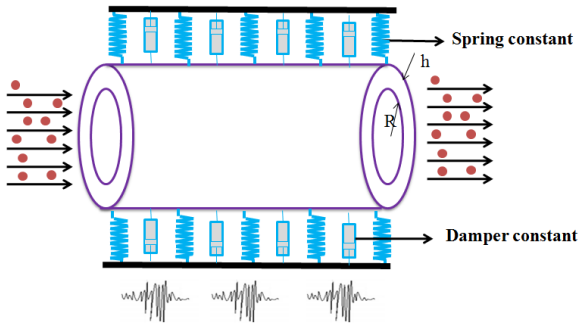

Fig. 1 Concrete pipe conveying nanoparticle-water in the soil under the earthquake load

motion are derived by energy method. Using Newmark and Galerkin methods, the dynamic stress, strain and displacement of the structure are obtained. The influences of internal fluid, nanoparticle volume percent, soil medium and damping of it are shown on the dynamic stress, strain and deflection of the pipe.

2. Mathematical model

In Fig. 1, a concrete pipe conveying water mixed by nanoparticles is shown which is buried in the soil considering damping of the soil. The pipe is under the axial seismic load.

Utilizing the higher order refined shear deformation theory of shell, the displacements are (Thai and Choi 2011)

$$U(x,\theta,z,t)=u(x,\theta,t)-z\frac{\partial}{\partial x}w_b(x,\theta,t)+z\left[\frac{1}{4}-\frac{5}{3}\left(\frac{z}{h}\right)^2\right]\frac{\partial}{\partial x}w_s(x,\theta,t), \tag{1}$$

$$V(x,\theta,z,t)=v(x,\theta,t)-z\frac{\partial}{R\partial\theta}w_b(x,\theta,t)+z\left[\frac{1}{4}-\frac{5}{3}\left(\frac{z}{h}\right)^2\right]\frac{\partial}{R\partial\theta}w_s(x,\theta,t), \tag{2}$$

$$W(x,\theta,z,t)=w_b(x,\theta,t)+w_s(x,\theta,t), \tag{3}$$

where (u,v) are the mid plane displacements along the (x, θ); w_s and w_b are shear and bending transverse deflections, respectively. The strain equations are

$$\varepsilon_{xx}=\frac{\partial u}{\partial x}-z\frac{\partial^2 w_b}{\partial x^2}-f\frac{\partial^2 w_s}{\partial x^2}, \tag{4}$$

$$\varepsilon_{\theta\theta}=\frac{\partial v}{\partial x}+\frac{w_b}{R}+\frac{w_s}{R}-z\frac{\partial^2 w_b}{R^2\partial\theta^2}-f\frac{\partial^2 w_s}{R^2\partial\theta^2}, \tag{5}$$

$$\gamma_{x\theta}=\frac{\partial v}{\partial x}+\frac{\partial u}{R\partial\theta}-2z\frac{\partial^2 w_b}{R\partial x\partial\theta}-2f\frac{\partial^2 w_s}{R\partial x\partial\theta}, \tag{6}$$

$$\gamma_{xz}=g\frac{\partial w_s}{\partial x}, \tag{7}$$

$$\gamma_{\theta z}=g\frac{\partial w_s}{R\partial\theta}, \tag{8}$$

where $f=-\frac{z}{4}+\frac{5}{3}z\left(\frac{z}{h}\right)^2$ and $g=\frac{5}{4}-5\left(\frac{z}{h}\right)^2$.

The stress-strain relations are

$$\begin{Bmatrix}\sigma_{xx}\\ \sigma_{\theta\theta}\\ \sigma_{\theta z}\\ \sigma_{zx}\\ \sigma_{x\theta}\end{Bmatrix}=\begin{bmatrix}C_{11}&C_{12}&0&0&0\\ C_{21}&C_{22}&0&0&0\\ 0&0&C_{44}&0&0\\ 0&0&0&C_{55}&0\\ 0&0&0&0&C_{66}\end{bmatrix}\begin{Bmatrix}\varepsilon_{xx}\\ \varepsilon_{\theta\theta}\\ \gamma_{\theta z}\\ \gamma_{xz}\\ \gamma_{x\theta}\end{Bmatrix}, \tag{9}$$

where C_{ij} $(i,j=1,2,\ldots,6)$ are stiffness coefficient.

2.1 Potential energy

The potential energy of the structure can be given as

$$\begin{aligned}U=\frac{1}{2}\int_{\Omega_0}\Bigg(&N_{xx}\frac{\partial u}{\partial x}+N_{\theta\theta}\left(\frac{\partial v}{\partial\theta}+\frac{w}{R}\right)\\&+Q_\theta\frac{\partial w_s}{R\partial\theta}+Q_x\frac{\partial w_s}{\partial x}+N_{x\theta}\left(\frac{\partial v}{\partial x}+\frac{\partial u}{R\partial\theta}\right)\\&+M^b_{xx}\frac{\partial^2 w_b}{\partial x^2}+M^b_{\theta\theta}\frac{\partial^2 w_b}{R^2\partial\theta^2}+M^b_{x\theta}\frac{\partial^2 w_b}{R\partial x\partial\theta}+\\&M^s_{xx}\frac{\partial^2 w_s}{\partial x^2}+M^s_{\theta\theta}\frac{\partial^2 w_s}{R^2\partial\theta^2}+M^s_{x\theta}\frac{\partial^2 w_s}{R\partial x\partial\theta}\Bigg)dxRd\theta,\end{aligned} \tag{10}$$

where the stress resultants may be written as

$$\begin{Bmatrix}N_i\\ M^b_i\\ M^s_i\end{Bmatrix}=\int_{-h/2}^{h/2}\begin{bmatrix}1\\ z\\ f\end{bmatrix}\sigma_i dz,\quad (\mathrm{i}=\mathrm{xx},\theta\theta,\mathrm{x}\theta) \tag{11}$$

$$Q_i=\int_{-h/2}^{h/2}g\sigma_i dz,\quad (\mathrm{i}=\mathrm{xz},\theta z) \tag{12}$$

2.2 Kinetic energy

The energy of kinetic for the structure can be expressed as

$$K=\frac{\rho}{2}\int_{\Omega_0}\int_{-h/2}^{h/2}\left(\left(\frac{\partial u}{\partial t}-z\frac{\partial^2 w_b}{\partial t\partial x}-f\frac{\partial^2 w_s}{\partial t\partial x}\right)^2+\left(\frac{\partial v}{\partial t}-z\frac{\partial^2 w_s}{R\partial t\partial\theta}-f\frac{\partial^2 w_s}{R\partial t\partial\theta}\right)^2+\left(\frac{\partial w_b}{\partial t}+\frac{\partial w_s}{\partial t}\right)^2\right)dV, \tag{13}$$

where ρ is the pipe density.

2.3 External work

Here, the work of the internal fluid, soil medium and earthquake load.

2.3.1 Internal fluid

The well-known Navier-Stokes equation can be written as

$$\rho_f\frac{d\mathbf{V}}{dt}=-\nabla\mathbf{P}+\mu\nabla^2\mathbf{V}+\mathbf{F}_{body}, \tag{14}$$

where $V \equiv (v_z, v_\theta, v_x)$ is the flow velocity vector in cylindrical coordinate system with components in longitudinal x, circumferential θ and radial z directions. Also, P, μ and ρ_f are the pressure, the viscosity and the density of the fluid, respectively and F_{body} denotes the body forces. In Navier-Stokes equation, the total derivative operator with respect to t is

$$\frac{d}{dt} = \frac{\partial}{\partial t} + v_x \frac{\partial}{\partial x} + v_\theta \frac{\partial}{R\partial\theta} + v_z \frac{\partial}{\partial z}, \tag{15}$$

At the point of contact between the fluid and the core, the relative velocity and acceleration in the radial direction are equal. So

$$v_z = \frac{dw}{dt}, \tag{16}$$

By employing Eqs. (15) and (16) and substituting into Eq. (14), the pressure inside the pipe can be computed as

$$\begin{aligned}\frac{\partial p_z}{\partial z} &= -\rho_f \left(\frac{\partial^2 w}{\partial t^2} + 2v_x \frac{\partial^2 w}{\partial x \partial t} + v_x{}^2 \frac{\partial^2 w}{\partial x^2} \right) \\ &+ \mu \left(\frac{\partial^3 w}{\partial x^2 \partial t} + \frac{\partial^3 w}{R^2 \partial\theta^2 \partial t} + v_x \left(\frac{\partial^3 w}{\partial x^3} + \frac{\partial^3 w}{R^2 \partial\theta^2 \partial x} \right) \right),\end{aligned} \tag{17}$$

By multiplying two sides of Eq. (17) in the inside area of the pipe (A), the radial force in the pipe is calculated as below

$$\begin{aligned}F_{fluid} = A\frac{\partial p_z}{\partial z} &= -\rho_f \left(\frac{\partial^2 w}{\partial t^2} + 2v_x \frac{\partial^2 w}{\partial x \partial t} + v_x{}^2 \frac{\partial^2 w}{\partial x^2} \right) \\ &+ \mu \left(\frac{\partial^3 w}{\partial x^2 \partial t} + \frac{\partial^3 w}{R^2 \partial\theta^2 \partial t} + v_x \left(\frac{\partial^3 w}{\partial x^3} + \frac{\partial^3 w}{R^2 \partial\theta^2 \partial x} \right) \right),\end{aligned} \tag{18}$$

Finally, the external work for the fluid pressure may be given as follows

$$\begin{aligned}W_f &= \int (F_{fluid}) w dA = \int \left(-\rho_{eff} \left(\frac{\partial^2 w}{\partial t^2} + 2v_x \frac{\partial^2 w}{\partial x \partial t} + v_x{}^2 \frac{\partial^2 w}{\partial x^2} \right) \right. \\ &\left. + \mu_{eff} \left(\frac{\partial^3 w}{\partial x^2 \partial t} + \frac{\partial^3 w}{R^2 \partial\theta^2 \partial t} + v_x \left(\frac{\partial^3 w}{\partial x^3} + \frac{\partial^3 w}{R^2 \partial\theta^2 \partial x} \right) \right) \right) w dA,\end{aligned} \tag{19}$$

where the effective viscosity ($\mu_{\mu_{eff}}$) and density ($\rho_{\mu_{eff}}$) for the water-nanoparticle flow are obtained utilizing mixture law for the Al_2O_3 nanoparticles with diameter of 13 nm as

$$\rho_{eff} = \phi\rho_n + (1-\phi)\rho_f, \tag{20}$$

$$\mu_{eff} = (1 + 39.11\varphi + 533.9\varphi^2)\mu_f, \tag{21}$$

where ρ_n, ρ_f, μ_n, μ_f and ϕ are density of nanoparticles, density of fluid, viscosity of nanoparticles, viscosity of fluid and nanoparticle volume percent respectively.

2.3.2 Soil medium

The work of the soil foundation is

$$W_s = \int_A \left(-k_s W - c_d \dot{W} \right) W dA, \tag{22}$$

where k_s is the soil spring coefficient and c_d is the damping of the soil foundation.

2.3.3 Earthquake load

The external work of the seismic force can be given as

$$W_e = \int_A \left(ma(\mathrm{t})\,\mathrm{u} \right) dA, \tag{23}$$

where $a(t)$ and m are the acceleration and mass, respectively.

2.4 Equations of motion

The equations of motion can be obtained using principal of Hamilton as

$$\int_0^t (\delta U - \delta W_f - \delta W - \delta W_e - \delta K) dt = 0. \tag{24}$$

By replacing Eqs. (10), (13), (19), (22) and (23) into Eq. (20), the equations of motion are

$$\begin{aligned}\delta u : \frac{\partial N_{xx}}{\partial x} + \frac{\partial N_{x\theta}}{R\partial\theta} &= I_0 \frac{\partial^2 u}{\partial t^2} - I_1 \frac{\partial^3 w_b}{\partial t^2 \partial x} \\ &- J_1 \frac{\partial^3 w_s}{\partial t^2 \partial x} + m a_x(\mathrm{t}),\end{aligned} \tag{25}$$

$$\delta v : \frac{\partial N_{x\theta}}{\partial x} + \frac{\partial N_{\theta\theta}}{R\partial\theta} = I_0 \frac{\partial^2 v}{\partial t^2} - I_1 \frac{\partial^3 w_b}{R\partial t^2 \partial\theta} - J_1 \frac{\partial^3 w_s}{R\partial t^2 \partial\theta}, \tag{26}$$

$$\begin{aligned}\delta w_b : &\frac{\partial^2 M_{xx}^b}{\partial x^2} + 2\frac{\partial^2 M_{x\theta}^b}{R\partial x \partial\theta} + \frac{\partial^2 M_{\theta\theta}^b}{R^2 \partial\theta^2} - \frac{N_{\theta\theta}}{R} \\ &+ P_{Fluid} - k_s (w_b + w_s) - c_d (\dot{w}_b + \dot{w}_s) = \\ &I_0 \left(\frac{\partial^2 w_b}{\partial t^2} + \frac{\partial^2 w_s}{\partial t^2} \right) + I_1 \left(\frac{\partial^3 u}{\partial t^2 \partial x} + \frac{\partial^3 v}{R\partial t^2 \partial\theta} \right) \\ &- I_2 \nabla^2 \left(\frac{\partial^2 w_b}{\partial t^2} \right) - J_2 \nabla^2 \left(\frac{\partial^2 w_s}{\partial t^2} \right),\end{aligned} \tag{27}$$

$$\begin{aligned}\delta w_s : &\frac{\partial^2 M_{xx}^s}{\partial x^2} + 2\frac{\partial^2 M_{x\theta}^s}{R\partial x \partial\theta} + \frac{\partial^2 M_{\theta\theta}^s}{R^2 \partial\theta^2} - \frac{N_{\theta\theta}}{R} \\ &+ \frac{\partial Q_{xz}}{\partial x} + \frac{\partial Q_{x\theta}}{R\partial\theta} + P_{Fluid} - c_d (\dot{w}_b + \dot{w}_s) = \\ &I_0 \left(\frac{\partial^2 w_b}{\partial t^2} + \frac{\partial^2 w_s}{\partial t^2} \right) + I_1 \left(\frac{\partial^3 u}{\partial t^2 \partial x} + \frac{\partial^3 v}{R\partial t^2 \partial\theta} \right) \\ &- J_2 \nabla^2 \left(\frac{\partial^2 w_b}{\partial t^2} \right) - K_2 \nabla^2 \left(\frac{\partial^2 w_s}{\partial t^2} \right),\end{aligned} \tag{28}$$

where

$$I_i = \int_{-h/2}^{h/2} \rho z^i dz \qquad (i = 0,1,2), \tag{29}$$

$$J_i = -\frac{1}{4} I_i + \frac{5}{3h^2} I_{i+2} \qquad (i = 1,2), \tag{30}$$

$$K_2 = \frac{1}{16} I_2 - \frac{5}{6h^2} I_4 + \frac{25}{9h^4} I_6. \tag{31}$$

In addition, the stress resultants are calculated in Appendix A.

3. Method of solution

Using the method suggested by Galerkin (Zamani Nouri

2018c) we have

$$\mathbf{d}=\begin{Bmatrix} u \\ v \\ w_b \\ w_s \end{Bmatrix}=\sum_{m=0}^{\infty}\sum_{n=0}^{\infty}\begin{Bmatrix} A_1\cos(\frac{m\pi x}{a})\sin(n\theta)\cos(\omega t) \\ A_2\sin(\frac{m\pi x}{a})\cos(n\theta)\cos(\omega t) \\ A_3\sin(\frac{m\pi x}{a})\sin(n\theta)\cos(\omega t) \\ A_4\sin(\frac{m\pi x}{a})\sin(n\theta)\cos(\omega t) \end{Bmatrix}, \quad (32)$$

where ω is frequency, n and m are circumferential and half axial wave numbers, respectively. Finally, the motion equations are

$$\left([K]\{d\}+[C]\{\dot{d}\}+[M]\{\ddot{d}\}\right)=\{F\}, \quad (33)$$

where $[K]$, $[C]$ and $[M]$ are the stiffness matrix, damping matrix and mass matrix, respectively. Also, $\{d\}=\{u,v,w_b,w_s\}$ is the displacement vector. Using the method of Newmark (Simsek 2010), Eq. (33) may be expressed as

$$\begin{aligned}&[K_L+K_{NL}(d_{i+1})+\alpha_0 M+\alpha_1 C](d_{i+1})= \\ &\left[Q_{i+1}+M\left(\alpha_0 d_i+\alpha_2\dot{d}_i+\alpha_3\ddot{d}_i\right)\right. \\ &\left.+C\left(\alpha_1 d_i+\alpha_4\dot{d}_i+\alpha_5\ddot{d}_i\right)\right],\end{aligned} \quad (34)$$

where subscript i+1 shows the time $t=t_{i+1}$; $\dot{d}$ and $\ddot{d}$ are structure velocity and structure acceleration which are

$$\ddot{d}_{i+1}=\alpha_0(d_{i+1}-d_i)-\alpha_2\dot{d}_i-\alpha_3\ddot{d}_i, \quad (35)$$

$$\dot{d}_{i+1}=\dot{d}_i+\alpha_6\ddot{d}_i+\alpha_7\ddot{d}_{i+1}, \quad (36)$$

where

$$\begin{aligned}&\alpha_0=\frac{1}{\chi\Delta t^2},\ \alpha_1=\frac{\gamma}{\chi\Delta t},\ \alpha_2=\frac{1}{\chi\Delta t},\ \alpha_3=\frac{1}{2\chi}-1, \\ &\alpha_4=\frac{\gamma}{\chi}-1,\ \alpha_5=\frac{\Delta t}{2}\left(\frac{\gamma}{\chi}-2\right),\ \alpha_6=\Delta t(1-\gamma),\ \alpha_7=\Delta t\gamma,\end{aligned} \quad (37)$$

in which γ=0.5 and χ=0.25. Using the iteration method, Eq. (33) may be analyzed.

4. Numerical results

Here, a concrete pipe with Young's modulus of E=20 GPa and Poisson's ratio of ν=0.3 is considered which has length to diameter ratio L/D=1 and ratio of pipe thickness to pipe radius of h/R=0.01. The internal fluid flow is water with density of ρ_f=998.2 kg/m^3 and viscosity of μ_f=1.003×10^{-3} Ns/m^2 and the nanoparticles in the fluid are Al_2O_3 with density of ρ_f=3970 kg/m^3. It should be noted that the spring constant of soil medium is calculated by the following relations (Bowles 1988)

$$k_s=\frac{2E_s}{\left(1-\nu_s^2\right)+2H/B} \quad (38)$$

where E_s and ν_s are soil Young's modulus and soil Poisson's ratio, respectively; B and H are width and height of the soil, respectively.

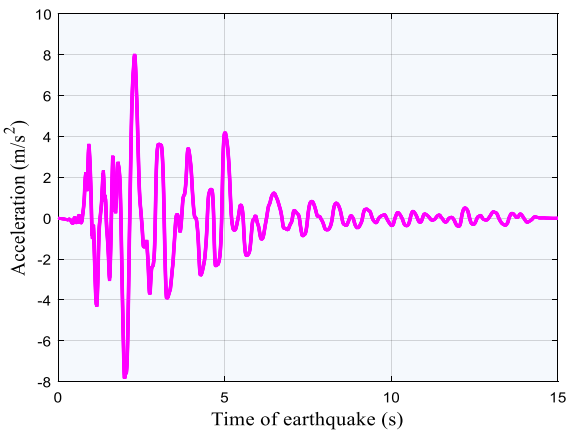

Fig. 2 Acceleration of Kobe earthquake

Table 1 Comparison of this work

Mode	Theory	Nondimensional frequency
1	Higher order theory, Ref. (2008)	75.2498
	Higher order theory, This work	75.3341
2	Higher order theory, Ref. (2008)	143.5110
	Higher order theory, This work	143.4821

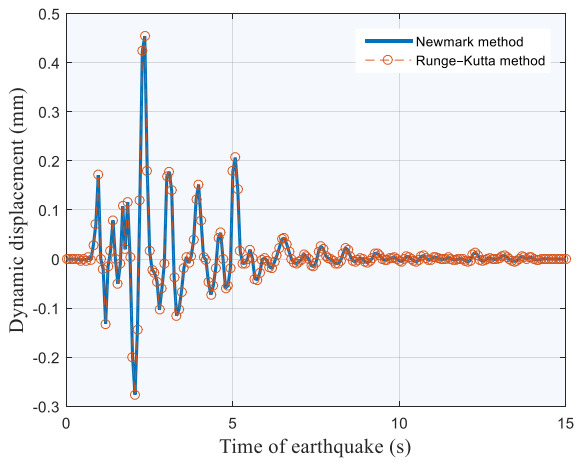

Fig. 3(a) The influence of volume fraction of nanoparticle on the dynamic displacement

The earthquake location is Kobe with the acceleration shown in Fig. 2.

4.1 Validation

The results of this paper are validated with the work of Pradyumna and Bandyopadhyay (2008) neglecting fluid, soil foundation and earthquake load. The dimensionless frequency ($\Omega=\omega L^2\sqrt{\rho_m/D_m}$) with $D_m=E_m h^3/\left[12(1-\nu_m^2)\right]$ is shown in Table 1. It is found that the results of this paper are close to the work of Pradyumna and Bandyopadhyay (2008).

For verifying the results of this paper without eliminating the parameters, the Runge-Kutta method is used and the obtained results are validated with Newmark methods applied in this article. The results of validation for dynamic displacement, strain and stress are shown in Figs.

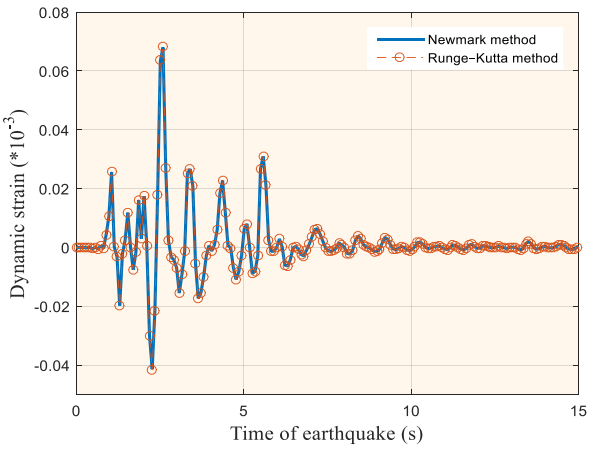

Fig. 3(b) The influence of volume fraction of nanoparticle on the dynamic strain

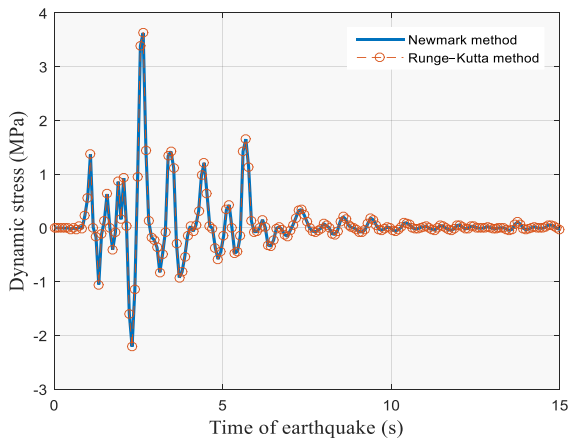

Fig. 3(c) The influence of volume fraction of nanoparticle on the dynamic stress

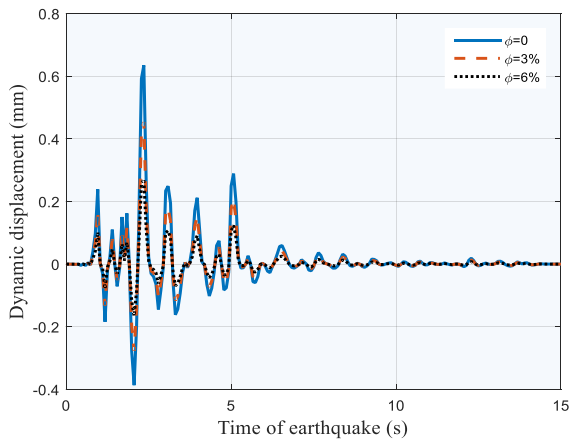

Fig. 4(a) The influence of volume fraction of nanoparticle on the dynamic displacement

3(a)-3(c), respectively. As can be seen, the results of two methods are close to each others which indicate the accuracy of obtained results in this work.

4.2 The effects of different parameters

Figs. 4(a)-4(c) show the influence of volume fraction of

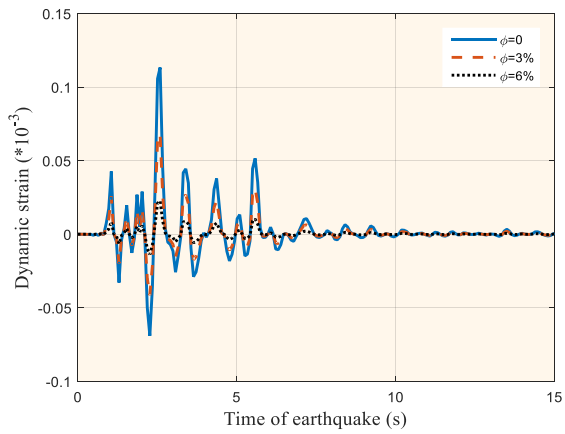

Fig. 4(b) The influence of volume fraction of nanoparticle on the dynamic strain

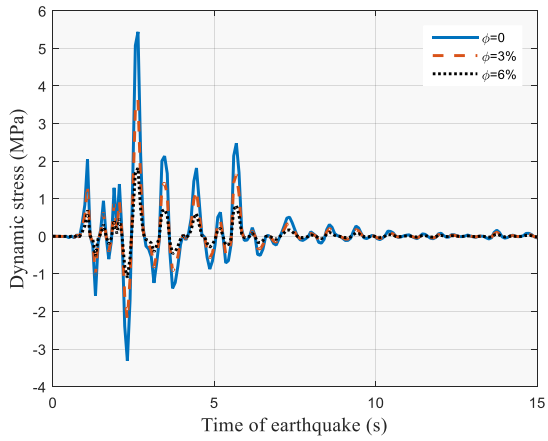

Fig. 4(c) The influence of volume fraction of nanoparticle on the dynamic stress

nanoparticle on the dynamic stress, strain and displacement, respectively. It is found that with enhancing the volume fraction of nanoparticle, the dynamic stress, strain and displacement are decreased. It is since with enhancing the nanoparticle volume percent in fluid, the pipe instability of is decreased. It is found that with enhancing the volume fraction of nanoparticle up to 3%, the dynamic stress, strain and deflection is decreased about 50%.

Figs. 5(a)-5(c) present respectively the soil medium influence on the dynamic stress, strain and displacement. Two cases for the soil medium (type of loose sand) are considered as soil medium without damping (k_s=4800 N/m^3, c_d=0) and with damping (k_s=4800 N/m^3, c_d=1000 Ns/m^2). The results present that with considering the soil medium, the dynamic stress, strain and displacement are decreased due to increase in the stiffness of the structure. In addition, considering damping of the soil reduces the dynamic stress, strain and displacement due to induce of active damp in the structure.

The influence of fluid on the dynamic stress, strain and displacement of the structure is presented in Figs. 6(a)-6(c), respectively. As can be found, with considering internal fluid in the concrete pipe, the dynamic stress, strain and deflection are increased. It is since with considering internal fluid flow in the concrete pipe, an internal force due to the

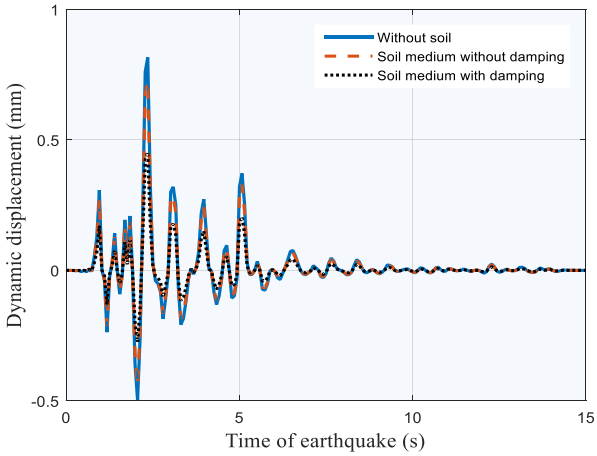

Fig. 5(a) The influence of soil medium on the dynamic displacement

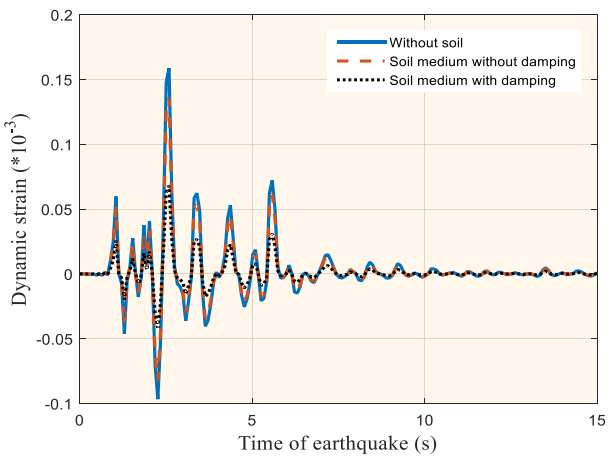

Fig. 5(b) The influence of soil medium on the dynamic strain

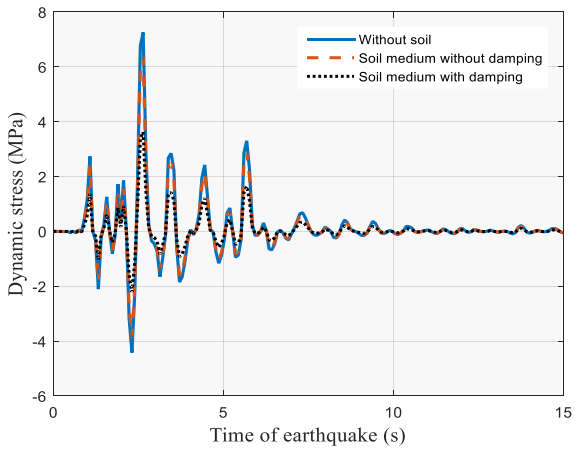

Fig. 5(c) The influence of soil medium on the dynamic stress

fluid will be induced in the pipe.

Fig. 7(a)-7(c), respectively, indicate the effect of length to diameter ratio of the concrete pipe on the dynamic stress, strain and deflection of the structure. The results show that with enhancing the length to diameter ratio of the concrete pipe, the dynamic stress, strain and deflection enhance. It is

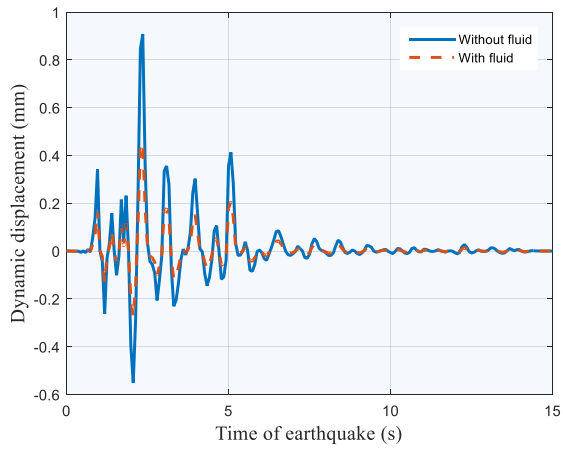

Fig. 6(a) The influence of fluid on the dynamic displacement

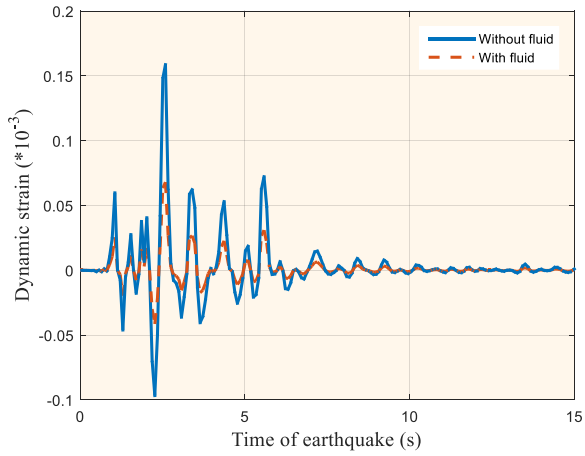

Fig. 6(b) The influence of fluid on the dynamic strain

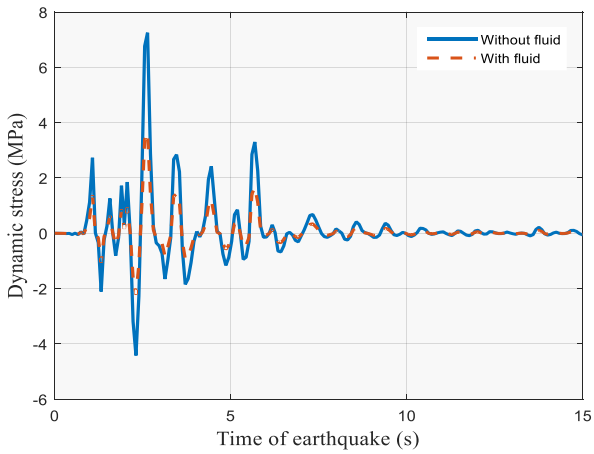

Fig. 6(c) The influence of fluid on the dynamic stress

because with enhancing the length to diameter ratio of the concrete pipe, the stiffness reduces.

5. Conclusions

Dynamic stress, strain and deflection in the concrete pipe conveying fluid-nanoparticle mixture were presented

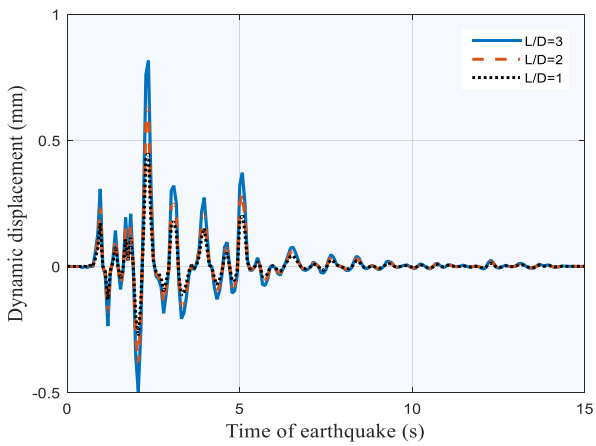

Fig. 7(a) The influence of length to diameter ratio of the pipe on the dynamic displacement

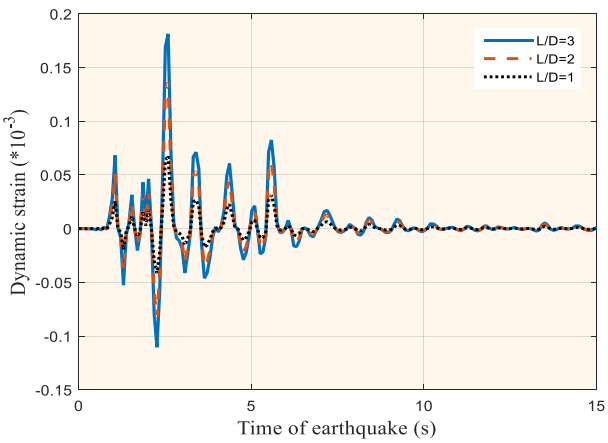

Fig. 7(b) The influence of length to diameter ratio of the pipe on the dynamic strain

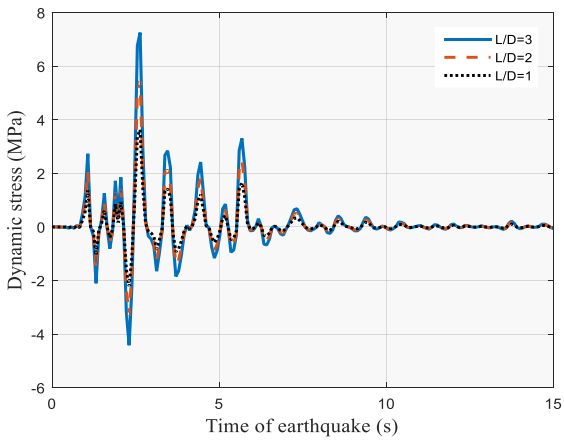

Fig. 7(c) The influence of length to diameter ratio of the pipe on the dynamic stress

in this paper. The concrete pipe was buried by the soil medium which was modeled by spring and damper elements. The equation of Navier-Stokes was applied for calculating the force induced by fluid. Utilizing refined higher order shear deformation theory of shell, the pipe was modeled and the motion equations were derived by energy method. Using Newmark and Galerkin methods, the dynamic stress, strain and displacement of the concrete pipe was calculated. The influences of the nanoparticle volume percent, fluid, length to diameter ration of the pipe, soil foundation and damping of it were assumed. It was found that with enhancing the nanoparticle volume fraction up to 3%, the dynamic stress, strain and deflection was decreased about 50%. It was obvious that with assuming the soil, the dynamic stress, strain and displacement are decreased. In addition, with considering internal fluid in the concrete pipe, the dynamic stress, strain and deflection were increased. Furthermore, with enhancing the length to diameter ratio of the concrete pipe, the dynamic stress, strain and deflection enhance.

References

Allahdadian, S. and Boroomand, B. (2016), "Topology optimization of planar frames under seismic loads induced by actual and artificial earthquake records", *Eng. Struct.*, **115**, 140-154. https://doi.org/10.1016/j.engstruct.2016.02.022.

Belardinelli, M.E., Bizzarri, A. and Cocco, M. (2003), "Earthquake triggering by static and dynamic stress changes", *J. Geophys. Res: Soild Earth Ban.*, **108**, 823-834. https://doi.org/10.1029/2002JB001779.

Bowles, J.E. (1988), *Foundation Analysis and Design*, USA.

Ding, Y., Ma, R., Shi, Y.D. and Li, Zh.X. (2018), "Underwater shaking table tests on bridge pier under combined earthquake and wave-current action", *Marine Struct.*, **58**, 301-320. https://doi.org/10.1016/j.marstruc.2017.12.004.

El-Helou, R.G. and Aboutaha, R.S. (2015), "Analysis of rectangular hybrid steel-GFRP reinforced concrete beam columns", *Comput. Concrete*, **16**, 245-260. https://doi.org/10.12989/cac.2015.16.2.245.

He, F., Dai, H. and Wang, L. (2018), "Vortex-induced vibrations of a pipe subjected to unsynchronized support motions", *J. Marine Sci. Technol.*, **23**(4), 978-990. https://doi.org/10.1007/s00773-017-0526-y.

Hind, M.Kh., Mustafa, Ö., Talha, E. and Abdolbaqi, M.Kh. (2016), "Flexural behavior of concrete beams reinforced with different types of fibers", *Comput. Concrete*, **18**, 999-1018. https://doi.org/10.12989/cac.2016.18.5.999.

Kayen, R. (2017), "Seismic displacement of gently-sloping coastal and marine sediment under multidirectional earthquake loading", *Eng. Geolog.*, **227**, 84-92. https://doi.org/10.1016/j.enggeo.2016.12.009.

Kumar Mishra, S., Kumar Roy, B. and Chakraborty, S. (2013), "Reliability-based-design-optimization of base isolated buildings considering stochastic system parameters subjected to random earthquakes", *Int. J. Mech. Sci.*, **75**, 123-133. https://doi.org/10.1016/j.ijmecsci.2013.06.012.

Liu, J., Wu, M., Yang, Y., Yang, G., Yan, H. and Jiang, K. (2018), "Preparation and mechanical performance of graphene concrete platelet reinforced titanium nanocomposites for high temperature applications", *Comput. Concrete*, **22**, 355-363. https://doi.org/10.1016/j.jallcom.2018.06.148.

O'Leary, P.M. and Datta, S.K. (1985), "Dynamics of buried pipelines", *Soil Dyn. Earthq. Eng.*, **4**, 151-159. https://doi.org/10.1016/0261-7277(85)90009-9.

Pioldi, F., Salvi, J. and Rizzi, E. (2017), "Refined FDD modal dynamic identification from earthquake responses with Soil-Structure Interaction", *Int. J. Mech. Sci.*, **127**, 47-61. https://doi.org/10.1016/j.ijmecsci.2016.10.032.

Powell, G.H. (1978), "Seismic response analysis of above-ground pipelines", *Eqrth. Eng. Struct. Dyn.*, **6**, 157-165.

https://doi.org/10.1002/eqe.4290060204.

Pradyumna, S. and Bandyopadhyay, J.N. (2008), "Free vibration analysis of functionally graded curved panels using a higher-order finite element formulation", *J. Sound Vib.*, **318**, 176-192. https://doi.org/10.1016/j.jsv.2008.03.056.

Simsek, M. (2010), "Non-linear vibration analysis of a functionally graded Timoshenko beam under action of a moving harmonic load", *Compos. Struct.*, **92**, 2532-46. https://doi.org/10.1016/j.compstruct.2010.02.008.

Thai, H.T. and Choi, D.H. (2011), "A refined plate theory for functionally graded plates resting on elastic foundation", *Compos. Sci. Technol.*, **71**, 1850-1858. https://doi.org/10.1016/j.compscitech.2011.08.016.

Wang, Zh., Yang, Y., Yu, H.S. and Muraleetharan, K.K. (2018), "Numerical simulation of earthquake-induced liquefactions considering the principal stress rotation", *Soil Dyn. Earthq. Eng.*, **90**, 432-441. https://doi.org/10.1016/j.soildyn.2016.09.004.

Wu, X., Lu, H., Huang, K., Wu, Sh. and Qiao, W. (2015), "Frequency spectrum method-based stress analysis for oil pipelines in earthquake disaster areas", *PLoS One*, **10**, e0115299. https://doi.org/10.1371/journal.pone.0115299.

Zamani Nouri, A. (2017), "Mathematical modeling of concrete pipes reinforced with CNTs conveying fluid for vibration and stability analyses", *Comput. Concrete*, **19**, 325-331. https://doi.org/10.12989/cac.2017.19.3.325.

Zamani Nouri, A. (2018a), "The effect of Fe_2O_3 nanoparticles instead cement on the stability of fluid-conveying concrete pipes based on exact solution", *Comput. Concrete*, **21**, 31-37. https://doi.org/10.12989/cac.2018.21.1.031.

Zamani Nouri, A. (2018b), "Vibration analysis of silica nanoparticle-reinforced concrete pipes filled with compressible fluid surrounded by soil foundation", *Struct. Concrete*, **19**(4), 1195-1201. https://doi.org/10.1002/suco.201700185.

Zamani Nouri, A. (2018c), "Seismic response of soil foundation surrounded Fe_2O_3 nanoparticles reinforced concrete pipes conveying fluid", *Soil Dyn. Earthq. Eng.*, **106**, 53-59. https://doi.org/10.1016/j.soildyn.2017.12.009.

Zhao, Ch., Chen, J., Wang, J., Yu, N. and Xu, Q. (2017), "Seismic mitigation performance and optimization design of NPP water tank with internal ring baffles under earthquake loads", *Nucl. Eng. Des.*, **318**, 182-201. https://doi.org/10.1016/j.nucengdes.2017.04.023.

CC

Appendix A

Substituting Eq. (9) into Eqs. (11) and (12), the stress resultants are

$$\begin{bmatrix} N_{xx} \\ N_{\theta\theta} \\ N_{x\theta} \\ M^b_{xx} \\ M^b_{\theta\theta} \\ M^b_{x\theta} \\ M^s_{xx} \\ M^s_{\theta\theta} \\ M^s_{x\theta} \end{bmatrix} = \begin{bmatrix} A_{11} & A_{12} & 0 & B_{11} & B_{12} & 0 & B^s_{11} & B^s_{12} & 0 \\ A_{12} & A_{22} & 0 & B_{12} & B_{22} & 0 & B^s_{12} & B^s_{22} & 0 \\ 0 & 0 & A_{66} & 0 & 0 & B_{66} & 0 & 0 & B^s_{66} \\ B_{11} & B_{12} & 0 & D_{11} & D_{12} & 0 & D^s_{11} & D^s_{12} & 0 \\ B_{12} & B_{22} & 0 & D_{12} & D_{22} & 0 & D^s_{12} & D^s_{22} & 0 \\ 0 & 0 & B_{66} & 0 & 0 & D_{66} & 0 & 0 & D^s_{66} \\ B^s_{11} & B^s_{12} & 0 & D^s_{11} & D^s_{12} & 0 & H^s_{11} & H^s_{12} & 0 \\ B^s_{12} & B^s_{22} & 0 & D^s_{12} & D^s_{22} & 0 & H^s_{12} & H^s_{22} & 0 \\ 0 & 0 & B^s_{66} & 0 & 0 & D^s_{66} & 0 & 0 & H^s_{66} \end{bmatrix} \begin{bmatrix} \partial u / \partial x \\ \partial v / \mathrm{R}\,\partial\theta \\ \partial u / \mathrm{R}\,\partial\theta + \partial v / \partial x \\ -\partial^2 w_b / \partial x^2 \\ -\partial^2 w_b / \mathrm{R}^2 \partial\theta^2 \\ -2\partial^2 w_b / \mathrm{R}\,\partial\theta\partial x \\ -\partial^2 w_s / \partial x^2 \\ -\partial^2 w_s / \mathrm{R}^2 \partial\theta^2 \\ -2\partial^2 w_s / \mathrm{R}\,\partial\theta\partial x \end{bmatrix}, \tag{A1}$$

$$\begin{bmatrix} Q_{\theta z} \\ Q_{xz} \end{bmatrix} = \begin{bmatrix} A^s_{44} & 0 \\ 0 & A^s_{55} \end{bmatrix} \begin{bmatrix} -\partial w_s / \mathrm{R}\,\partial\theta \\ -\partial w_s / \partial x \end{bmatrix}, \tag{A2}$$

where

$$\left(A_{ij}, B_{ij}, D_{ij}, E_{ij}, F_{ij}, H_{ij}\right) = \int_{-h/2}^{h/2} \left(1, z, z^2, z^3, z^4, z^5, z^6\right) C_{ij} dz, \quad (i, j = 1,2,4,5,6) \tag{A3}$$

$$B^s_{ij} = -\frac{1}{4}\mathrm{B}_{ij} + \frac{5}{3h^2} E_{ij}, \tag{A4}$$

$$D^s_{ij} = -\frac{1}{4} D_{ij} + \frac{5}{3h^2} F_{ij}, \tag{A5}$$

$$H^s_{ij} = \frac{1}{16} D_{ij} - \frac{5}{6h^2} F_{ij} + \frac{25}{9h^4} H_{ij}, \tag{A6}$$

$$A^s_{ij} = \frac{25}{16} A_{ij} - \frac{25}{2h^2} D_{ij} + \frac{25}{h^4} F_{ij}, \tag{A7}$$